Contributed paper

OPTO-ELECTRONICS REVIEW 7(4), 297–303 (1999)

Low-cost 320×240 uncooled IRFPA using conventional silicon IC process

T. ISHIKAWA*, M. UENO, K. ENDO, Y. NAKAKI, H. HATA, T. SONE, and M. KIMATA

Advanced Technology R&D Center, Mitsubishi Electric Corporation
4–1, Mizuhara, Itami, Hyogo, 664–8641, Japan

A 320×240 uncooled infrared focal plane array (IRFPA) with series PN junction diodes fabricated on a silicon-on-insulator (SOI) wafer has been developed. Resistive bolometers, pyroelectric detectors and thermopile detectors have been reported for large scale uncooled IRFPAs, while the detector developed uses the temperature dependence of forward-biased voltage of the diode. The diode has low 1/f noise because it is fabricated on the monocrystalline SOI film which has few defects. The diode is supported by buried silicon dioxide (BOX) film of the SOI wafer, which becomes a part of a thermal isolated structure by using bulk silicon micromachining technique. The detector contains an absorbing membrane with a high fill factor of 90% to achieve high IR absorption, and the readout circuit of the FPA contains a gate modulation integrator to suppress the noise. Low cost IRFPA can be supplied because the whole structure of the FPA is fabricated on commercial SOI wafers using a conventional silicon IC process.

Keywords: uncooled IRFPA, SOI, PN junction diode, forward-biased characteristics, fill factor, silicon compatible process.

1. Introduction

In the past several years, a large number of uncooled infrared (IR) FPAs have been developed using silicon IC process and micromachining technique. Large scale FPAs generally use resistive bolometers, pyroelectric detectors and thermopile detectors to sense IR radiation. For example, vanadium oxide [1] as a resistive bolometer material and $Ba_{1-x}Sr_xTiO_3$ (BST) [2] as a pyroelectric material exhibit high temperature dependence of electrical properties (resistance, polarization and so on); therefore, FPAs with these materials have achieved high responsivity. In general, the readout integrated circuits of IRFPAs are manufactured using standard silicon IC process. However, the detectors with these materials are not compatible with the silicon process because the materials are uncommon for silicon IC devices. For low-cost uncooled FPAs, it is very advantageous if they can be manufactured using only silicon process over the whole production. Silicon PN junction diodes, which are devices compatible with the silicon process, can be applied to a thermal detector with its temperature dependence of the electrical properties. A polycrystalline Si diode deposited by CVD technique was used for a thermal detector [3,4]. The problem is that deposited Si films have been reported to exhibit large 1/f noise [5].

We have developed an uncooled IRFPA with series diodes that have been fabricated on a silicon-on-insulator (SOI) film instead of the deposited Si film. It was expected that the fewer defects or localized states of the SOI film would reduce the 1/f noise. Also, the detector contains an absorbing membrane with a high fill factor to achieve high IR absorption, and the readout circuit of the FPA contains a gate modulation integrator to suppress the noise.

In this paper, we describe the detector structure, the detector diode properties, the readout circuit design and the performance of the FPA.

*e-mail: toishika@lsi.melco.co.jp

2. Detector design

2.1. Thermal detector structure using SOI

Figure 1 shows a commercial SOI wafer structure, which consists of two single-crystal silicon regions separated by an insulating film. The sandwiched insulator is silicon dioxide and referred to as the buried oxide (BOX).

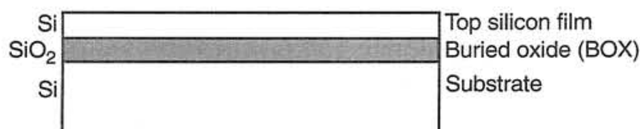

Fig. 1. SOI wafer structure.

Figure 2 shows a cross sectional structure of the thermal detector using the SOI wafer. The PN junction diode is fabricated on the SOI film, and the eight PN junctions are connected in series in order to improve the temperature coefficient. The diode is thermally isolated from the supporting bulk silicon substrate to achieve low thermal conductance. The BOX film and the passivation film over the diode protect the diode while etching the bulk silicon substrate. Two support legs from which the diode is suspended contain local interconnections to connect readout circuits. Excellent thermal isolation was achieved by a microbridge structure with a thermal conductance of 8.2×10^{-8} W/K.

A conventional microbolometer pixel has a thin detector plate supported over a readout circuit using microbridge structures. One of the difficulties of the microbridge structures is the limited fill factor, because the detector area is reduced by the support legs. In order to overcome this disadvantage, we have developed a new infrared absorbing structure. The structure includes an absorbing membrane which is expanded over the diode to achieve a high fill factor. The membrane consists of two metallic layers separated by an insulating film. The bottom metal serves as an infrared reflector and the top metal serves as an infrared absorber with a sheet resistivity of about 377 Ω/square. The sandwiched insulating film is constructed with silicon dioxide and silicon nitride layers of which the thickness is designed to maximize the absorption in the wavelength range between 8 and 12 μm. Amorphous Si is used as a sacrificial layer, which is located between the absorbing membrane and the passivation films on the SOI diode. Figure 3 shows a surface and bulk micromachining process flow of the SOI thermal detector. The sacrificial Si layer and the bulk Si substrate under the diode are finally removed by etching to form a thermally isolated structure with a high fill factor absorbing membrane. The high fill factor and the low thermal conductance have made it possible to develop a large scale uncooled IRFPA with a pixel number of 320×240 and a pixel pitch of 40 μm. The SOI diode pixel array with 40 μm pitch is shown in Fig. 4.

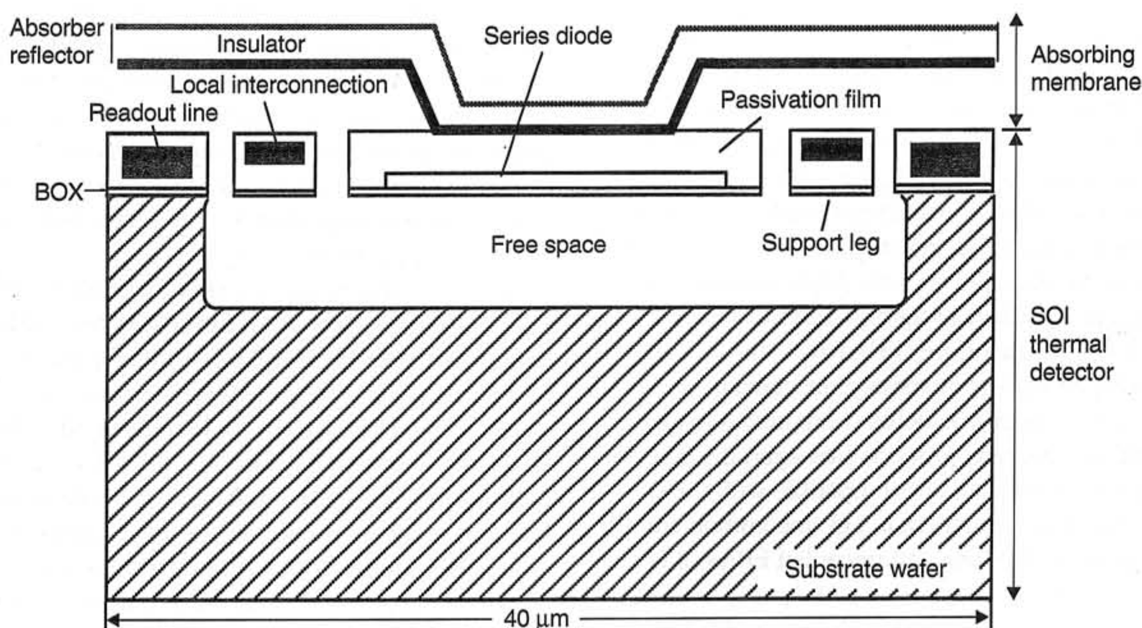

Fig. 2. Cross sectional structure of SOI diode pixel with infrared absorbing structure.

 © 1999 COSiW SEP, Warsaw

SOI diode

Substrate

○ 1st via hole etching to substrate

Amorphous Si

○ Amorphous Si deposition
for sacrificial layer

Absorbing membrane

○ Absorbing membrane fabrication

○ 2nd via hole ething to sacrificial layer

Free space

○ Removing sacrificial layer and substrate

Fig. 3. Process flow of SOI thermal detector with absorbing membrane.

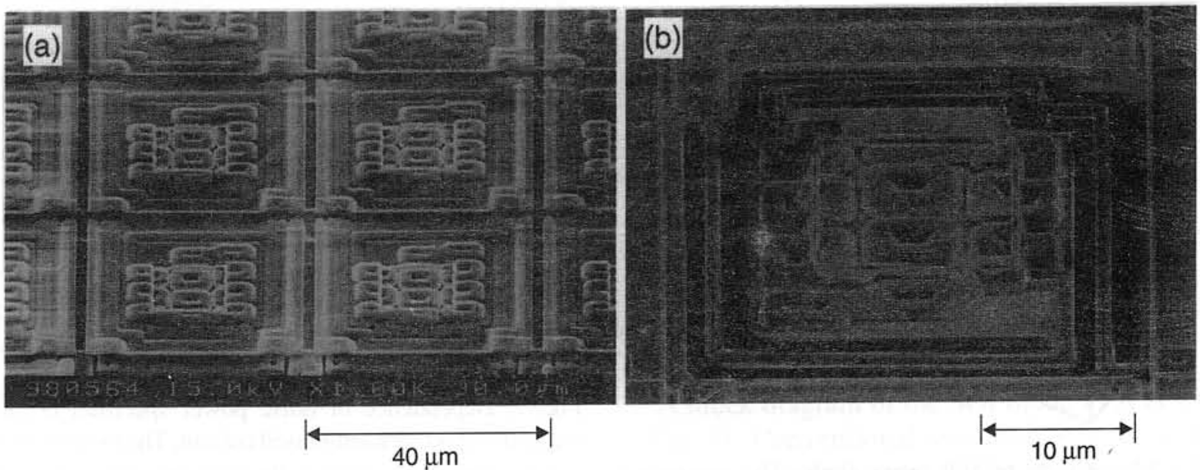

Fig. 4. SEM photographs of SOI diode pixels with (a) and without (b) absorbing membrane.

2.2. Characteristics of series diode

The detector in this work has a series diode which is constructed with lateral PN junction diodes serially connected by metal straps as shown in Fig. 5. The forward current of the series diode (I_f) [6] is given by

$$I_f = I_s \exp\left(\frac{qV_f}{nkT} - 1\right), \tag{1}$$

where I_s is the saturation current, n is the number of series, V_f is the forward-biased voltage across the series diode, k is the Boltzmann constant, q is the elementary charge, and T is the absolute temperature. The saturation current I_s, is also given by

$$I_s \cong T^{(3+\gamma/2)} \exp\left(-\frac{E_g}{kT}\right), \tag{2}$$

where E_g is the energy gap of Si and γ is the constant. Under the condition of a constant current, the temperature coefficient of V_f can be expressed as

$$\left.\frac{dV_f}{dT}\right|_{const\, I_f} = -n\left(\frac{[E_g + (3+\gamma/2)kT] - \frac{qV_f}{n}}{qT}\right) = -n\left(\frac{1.21 - \frac{V_f}{n}}{T}\right). \tag{3}$$

From equation (3), we know the temperature coefficient of V_f is proportional to the number of series. The relationship between the temperature coefficient of V_f and the number of series is shown in Fig. 6.

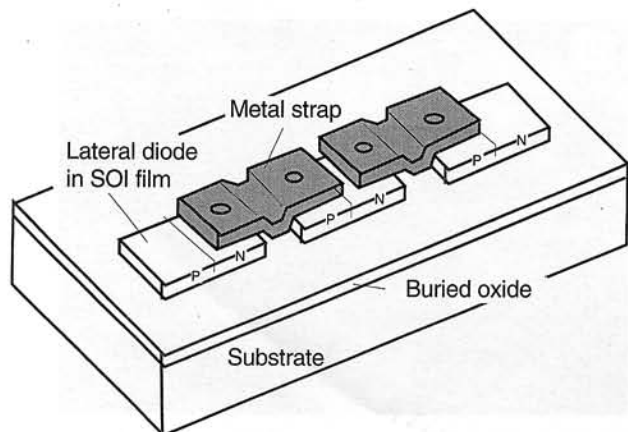

Fig. 5. Oblique view of SOI series diode. The number of series is three as an example.

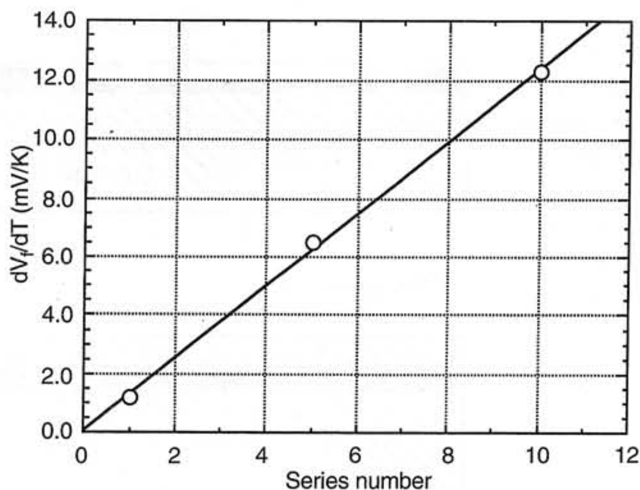

Fig. 6. Thermal coefficient of series diode vs number of series. The diode width is 5 μm and thickness is 0.14 μm. The forward bias current is 50 μA.

Diode noise principally consists of shot noise, thermal noise and 1/f noise. The power spectrum density of the shot noise (SI) is given by SI = $2qI_f$, which indicates that SI is proportional to I_f. The noise spectrum of the series diode is shown in Fig. 7. Although the diodes of polycrystalline and amorphous Si materials exhibit large 1/f noise, the noise of the SOI series diode is dominated by the shot noise and little 1/f noise. It is assumed that this phenomenon is caused by the higher quality of SOI film than that of the deposited polycrystalline and amorphous silicon ones.

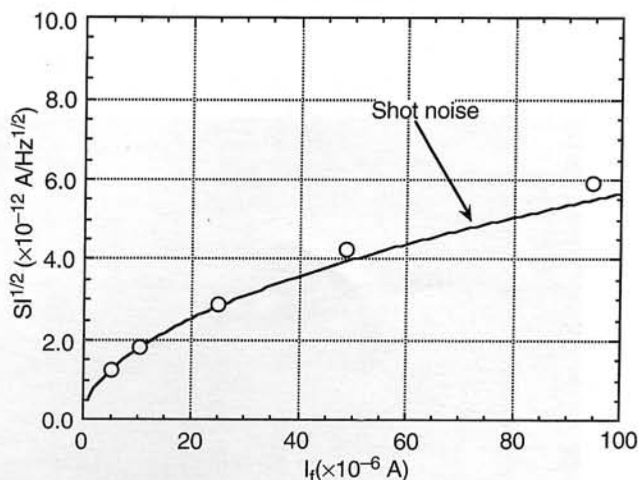

Fig. 7. Dependence of noise power spectrum density of series diode on forward-biased current. The number of series is five. The solid curve is the shot noise power spectrum density.

 © 1999 COSiW SEP, Warsaw

3. Circuit design

3.1. Gate modulation integrator

Since the series diode has a poorer temperature coefficient than the vanadium oxide, the noise of the readout circuit must be suppressed to get good performance of FPA. This FPA includes a gate modulation integrator [7] in each column for output signal amplification and bandwidth limitation. Figure 8 shows the readout circuit with the gate modulation integrator. The forward voltage temperature change of the diode modulates the gate voltage of the input transistor (Mi). The change of the forward voltage is integrated by discharging the integration capacitor (Cin) through the input transistor. Just after the integration, the output signal is read out. The integration capacitor is periodically reset to the reference level (Vref). The gain of this circuit is given by

$$Av = \frac{gmt_{\text{int}}}{C_{\text{int}}} \tag{4}$$

where gm is the transconductance of the input transistor, C_{int} is the capacitance of the integration capacitor, and t_{int} is the integration time. The gain and the dc level of the circuit are controlled by the source voltage (Vss) of the input transistor, while the bias current of the diode is controlled by the gate voltage of the load transistor (Mc). Figure 9 shows the dependence of responsivity and circuit output noise on the bias current of the diode. We can design the circuit parameters so that the forward voltage fluctuation of the diode dominates the output noise. The noise voltage of the diode depends on its bias current and dynamic resistance. When the bias current increases, the noise voltage is enhanced owing to the increase of the shot noise, whereas when the bias current decreases beyond a certain level, the noise voltage is also enhanced owing to the increase of the dynamic resistance of the diode. The noise is minimized under the current between 10^{-5} and 10^{-4} A, while the responsivity increases when the bias current is decreased. Therefore, the forward-bias current should be optimized to obtain the best S/N ratio. Figure 10 shows a noise equivalent temperature difference (NETD) estimation of this FPA. Under a current of 10 μA, we obtained the NETD of less than 0.2 K with f/1 optics, which was the best performance of our FPA.

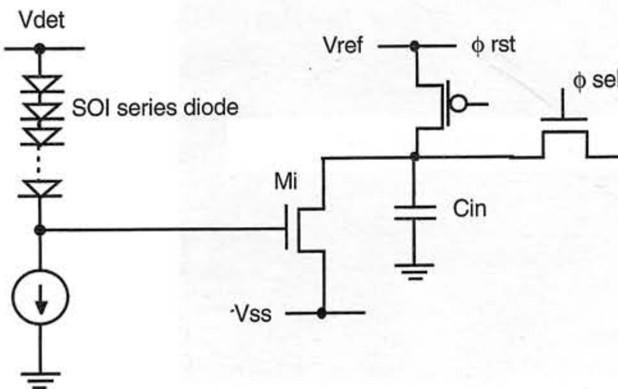

Fig. 8. Output circuit with gate modulation integrator.

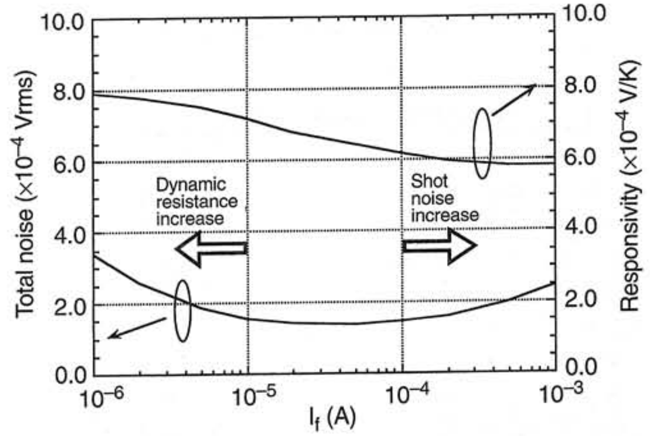

Fig. 9. Dependence of circuit output noise and responsivity on forward-biased current.

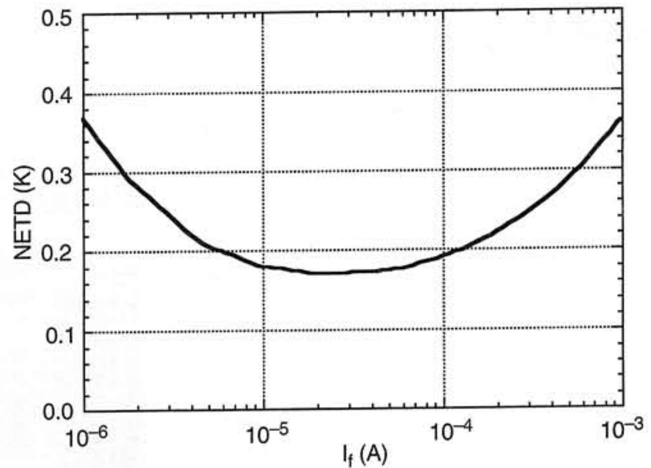

Fig. 10. Estimation of NETD.

3.2. Uncooled IRFPA using SOI diode

A block diagram of the SOI diode FPA is shown in Fig. 11. Conventional uncooled IRFPAs with bolometers or pyroelectric detectors need a switch transistor in each pixel, while this FPA has no ac-

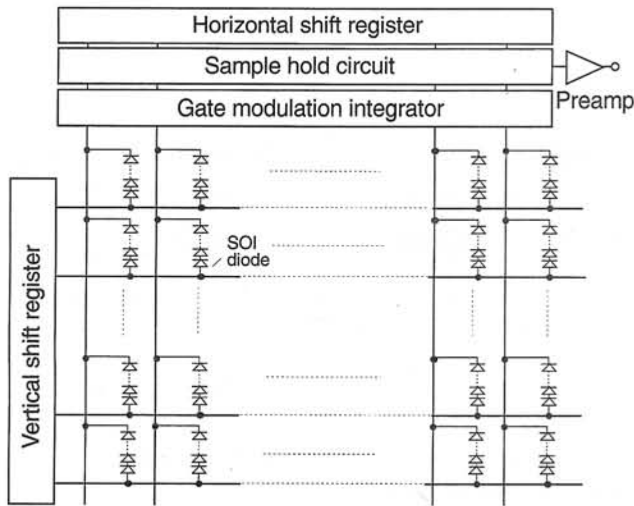

Fig. 11. Block diagram of SOI diode FPA.

tive elements because the PN junction in the pixel cuts off the current which would flow into unselected pixels [3]. In this readout circuit, when a selected series diode is biased through the vertical shift register, the current flows into the selected diodes. The signal generated from the diode enters the gate modulation integrator and is amplified about 10 times. The bandwidth of the signal is also limited to within 9 kHz in the integrator. Finally, each column is addressed by the horizontal shift register to put out the signal.

The chip photograph of the focal plane array is shown in Fig. 12. This FPA was fabricated on a 200-mm SOI wafer by using a ULSI process line. The specifications of the 320×240 uncooled FPA are summarized in Table 1.

Table 1. Specifications of 320×240 SOI diode uncooled FPA

Array configuration	320×240
Pixel size	40×40 μm^2
Detector thermal conductance	8.2×10^{-8} W/K
Temperature coefficient of series diode	–11 mV/K
Detector fill factor	90%
IR absorption	80%
Frame rate	60 Hz
Number of outputs	1
NETD (f/1)	0.2 K

5. Conclusion

We have developed an uncooled IRFPA with a PN junction diode which is fabricated on an SOI wafer. The pixel has no active elements except for the PN junction diode. The diode detects infrared rays as a change of the diode forward voltage. Since the diode is fabricated on SOI film, the 1/f noise is suppressed because of the excellent film quality. This FPA detector contains an absorbing membrane to obtain a high fill factor. The absorbing membrane of each pixel is expanded over the diode to achieve a fill factor of 90% and a pixel of 40 μm. The readout circuit of the FPA includes a gate modulation integrator to reduce the noise of the circuit. The signal is amplified about 10 times, and the bandwidth of the signal is limited to

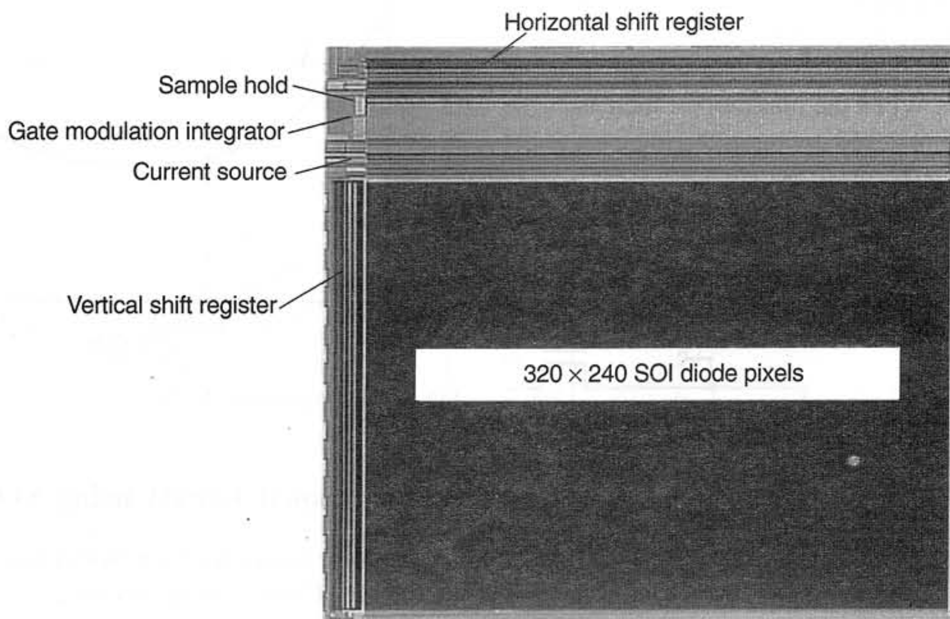

Fig. 12. Chip photograph of SOI diode FPA.

 © 1999 COSiW SEP, Warsaw

within 9 kHz in the integrator. Consequently, we have achieved an NETD of 0.2 K with a 320×240 element uncooled FPA having a small pixel of 40 μm square. Moreover, the whole structure of the FPA can be fabricated on commercial SOI wafers in silicon process plants. This makes it possible to reduce the production cost of IRFPAs to an acceptable level for wide application fields.

In this paper, we have described a diode detector which is fabricated on an SOI wafer. However, other silicon devices such as junction FETs, MOSFETs, and JFETs fabricated on SOI wafers can also be applied to thermal detectors, and it should be possible for these devices, too, to have higher responsivity because of the larger temperature dependence of their electric properties.

Acknowledgments

The authors would like to thank Y. Yamaguchi, T. Ipposhi, and S. Maegawa for helpful discussions about the SOI technology.

References

1. R.A. Wood, "Uncooled thermal imaging with monolithic silicon focal planes", *Proc. SPIE* **2020**, 322-329 (1993).
2. C. Hanson, "Uncooled thermal imaging at Texas Instruments", *Proc. SPIE* **2020**, 330-339 (1993).
3. M. Ueno, O. Kaneda, T. Ishikawa, K. Yamada, A. Yamada, M. Kimata, and M. Nunoshita, "Monolitic uncooled infrared image sensor with 160×120 pixels", *Proc. SPIE* **2552**, 636-643 (1995).
4. A. Tanaka, M. Suzuki, R. Asahi, R. Tabata, and S. Sugiyama, "Infrared linear image sensor using a poly-Si pn junction diode array", *Infrared Phys.* **33**, 229-236 (1992).
5. H. Wieczorek "1/f noise in amorphous silicon nip and pin diodes", *J. Appl. Phys.* **77**, 3300-3307 (1995).
6. S.M. Sze, in *Physics of Semiconductor Devices*, second edition, Chap.2, pp. 74-89, John Wiley & Sons, New York, 1981.
7. L.J. Kozłowski, S.L. Johnston, W.V. McLevige, A.H.B. Vanderwyck, D.E. Cooper, S.A. Cabelli, E.R. Blanzejewski, K. Vural, and W.E. Tennant "128×128 PACE-I HgCdTe hybrid FPAs for thermoelectrically cooled applications", *Proc. SPIE* **1685**, 193-204 (1992).